Journal of Thermal Analysis and Calorimetry (2023) 148:3073–3088
https://doi.org/10.1007/s10973-022-11408-2

Effect of nitrous oxide on laminar burning velocity, hydrodynamic, and diffusive–thermal instability of biogas combustion

Shehab Elhawary[1] · Aminuddin Saat[1] · Mazlan Abdul Wahid[1] · Mohd Zarhamdy Md Zain[1]

Received: 25 January 2022 / Accepted: 12 May 2022 / Published online: 16 June 2022

Abstract

Biogas is a potential alternative energy source with low environmental impact. However, the practical applications of biogas are relatively limited due to the existence of CO_2 which acts as a dilutant that decreases the calorific value and the burning rate of biogas. Nitrous oxide (N_2O) is known to be a powerful oxidizing agent for propulsion applications which can enhance the combustion rate of biogas. In the present paper, the laminar burning velocity (LBV), hydrodynamic instability, and diffusive–thermal instability of biogas/N_2O oxide were experimentally studied at different equivalence ratios. The spherical propagating premixed flames for various mixtures of biogas-N_2O were determined using the constant volume combustion vessel at 303 K and atmospheric pressure. Two mechanisms were used in CHEMKIN-PRO software in order to estimate the predicted combustion characteristics of biogas/N_2O mixtures. The results indicate that the decline in LBVs was prominent in the fuel-rich mixtures than in the fuel-lean mixtures with CO_2 dilution. It is found that the influence of curvature on the flame front is weakened at the fuel lean-to-stoichiometric mixture due to the decrease in the flame thickness; therefore, flame instability tends to increase at the lean-to-stoichiometric region. Thermal diffusivity values decline with increasing the CO_2% except in the equivalence ratios of $\varphi = 1.0$ and $\varphi = 1.4$, which showed no impact on the thermal diffusivity. The thermal reaction of N_2O decomposition is the most significant reaction in biogas/N_2O combustion at lean mixtures of $\varphi = 0.6$ and 0.8.

Keywords Laminar burning velocity · Nitrous oxide · Biogas · Diffusive · Thermal instabilities · Hydrodynamic instability · Alternative fuels

Introduction

The rapid increases in energy consumption joined with considerable concerns about climate change have led to more attention to renewable sources of energy and alternative fuels [1]. Biogas is one of the promising alternative fuels that can be produced easily from landfills and through anaerobic digestion. Methane (CH_4) and carbon dioxide (CO_2) are the main components of biogas with a small proportion of nitrogen, oxygen, and other organic compounds. The percentage of CH_4 in the biogas varies from 40 to 80% while the percentage of CO_2 varies from 20 to 60%. Due to the relatively high proportion of CO_2, the biogas fuel has a low burning rate and heating value, which could limit its practical applications in some industries that require high burning rate [2–4]. Therefore, the improvement in biogas combustion performance is needed in order to widen and develop its practical applications.

Nitrous oxide (N_2O) has been demonstrated to be a powerful, non-toxic, and non-corrosive oxidizing agent for rocket propulsion systems and space applications. N_2O can increase the burning rate of combustion due to its exothermal dissociation in fuel/N_2O mixtures. Although N_2O is considered a greenhouse gas, recent studies have revealed that N_2O can serve as a renewable energy source [5, 6].

The laminar burning velocity (LBV) is one of the fundamental characteristics of a reacting premixed mixture

✉ Shehab Elhawary
shehab_elhawary@yahoo.com

Aminuddin Saat
amins@mail.fkm.utm.my

Mazlan Abdul Wahid
mazlan@mail.fkm.utm.my

Mohd Zarhamdy Md Zain
zarhamdy@mail.fkm.utm.my

[1] High-Speed Reacting Flow Laboratory, School of Mechanical Engineering, Faculty of Engineering, Universiti Teknologi Malaysia, 81310 UTM Skudai, Johor, Malaysia

which is helpful for understanding important fundamental properties such as diffusivity, reactivity, and exothermicity. Accurate measurement of laminar burning velocity is important for the characterization of premixed combustion properties of the fuel and the development of new kinetic models. Understanding the laminar burning velocity variation with thermodynamic conditions is significant from the perspective of practical applications in industrial furnaces, gas turbine combustors, and rocket engines [7].

LBVs can be estimated by various techniques such as Bunsen burner [8], heat flux [9, 10], spherical flame [7, 11–14], flat flame [15], and counter flow [16]. Nitrous oxide flame propagation was studied under different conditions. Flame propagation measurements of CH_4/N_2O low-pressure flat flames were reported by Vanderhoff et al. [17] using laser Raman spectroscopy. The structure of premixed CH4/N_2O flame in the presence of O_2 or Ar was studied by Habeebullah et al. [18], Zabarnick [19], and Vandooren et al. [20] by measurements of stable and unstable species in flat flames at 30–50 torr. Flame structure investigations were used to validate different mechanisms developed for mixtures that contain N_2O.

Laminar burning velocities of N_2O with various fuels (CH_4, C_2H_2, C_3H_8, and H_2) diluted by N_2 were determined by Powell et al. [15, 21] using a McKenna flat flame burner at near-atmospheric pressure. The sensitivity studies and reaction path analyses were used in order to illustrate the important reactions. Pfahl et al.[22] determined the LBVs of CH_4/N_2O; however, these mixtures included other flammable components such as H_2 and NH_3. Shebeko et al. [23] investigated experimentally the influence of trifluoromethane on the LBV of near-limit mixtures of CH_4/N_2O. In the experimental study by Newman-Lehman et al.[24], non-premixed flames of CH_4/O_2 and C_2H_6/O_2 were replaced by CH_4/N_2O and C_2H_6/N_2O, respectively; it was found that O_2 replacement with N_2O inhibited the flame propagation. Domnina et al. [25] determined the laminar burning velocities of $CH_4/N_2O/N_2$ mixtures using closed vessel explosions, and from the detailed modeling of free laminar premixed flames, they indicated that N_2 addition to each CH_4/N_2O mixture results in the decrease in LBV along with the increase in flame width.

While there is significant interest in using biogas as an alternative to conventional fuels in multiple combustion applications [26], the presence of CO2 in biogas has limited its practical utilization in several applications that require high burning rates.

Nitrous oxide is a powerful oxidizing agent for rocket propulsion engines that can generate significant thrust. When decomposed, N_2O has a positive enthalpy of formation and can produce 82 kJ mol^{-1} as shown in Eq. 1. Therefore, in combustion reactions, N2O is a more powerful oxidant than pure oxygen (O2). As demonstrated in Eqs. 2 and 3, stoichiometric combustion of 1 mol CH_4 with N_2O generates about 30% more energy than stoichiometric combustion of 1 mol CH_4 with oxygen [27].

$$N_2O \rightarrow \frac{1}{2}O_2 + N_2,\ \Delta\hat{H}^{\circ}C = -82\ \text{kJ mol}^{-1} \quad (1)$$

$$CH_4 + 4N_2O \rightarrow CO_2 + 2H_2O + 4N_2,\ \Delta\hat{H}^{\circ}C = -1219\ \text{kJmol}^{-1} \quad (2)$$

$$CH_4 + 2O_2 \rightarrow CO_2 + 2H_2O,\ \Delta\hat{H}^{\circ}C = -890\ \text{kJmol}^{-1} \quad (3)$$

Therefore, N_2O is commonly employed to supercharge high-performance vehicles' engines and as an oxidizer in hybrid rocket engines in the aerospace industry. Hence, nitrous oxide could be used as an oxidizer to enhance the burning rate of biogas combustion and diminish the dilution effect of carbon dioxide to expand the utilization of biogas in propulsion applications.

Yet, there is a lack of studies that investigated the fundamental combustion characteristics of biogas/N_2O. The objective of this study is to investigate the fundamental combustion characteristics of biogas/N_2O mixtures in terms of laminar burning velocity and flame stability at various ranges of equivalence ratios.

Our findings show that the use of N_2O as an oxidizer has increased significantly the laminar burning velocity of biogas compared to biogas/air. In addition, it was found that nitrous oxide has a substantial effect on the flame stability of biogas, specifically at lean mixtures. This study may support the efficient performance of biogas in high burning applications in order to expand the potential of biogas as an alternative fuel.

Experimental setup

The experiments were performed in a cylindrical constant volume combustion vessel. The experimental platform is consisting of a constant volume chamber, high-speed camera (Phantom 7.1), temperature control system, ignition system, vacuum pump, exhaust system, and Data Acquisition System (DAQ). The chamber has an approximated volume of 30L with a 190-mm quartz window on both sides for optical access. Images of central propagating biogas/N_2O flame are captured using high-speed schlieren photography as shown in Fig. 1. The vacuum pump is used to maintain the vacuum down to 1×10^{-1} mbar in the combustion chamber. The ignition system is fitted with inductive–capacitive high-voltage sparks generated between two electrodes that provide ignition energy in the form of central point ignition with a spark gap of about 0.7 mm. Two thermocouples type K are employed to measure the ambient temperature of the internal reactants and another two thermocouples to determine the

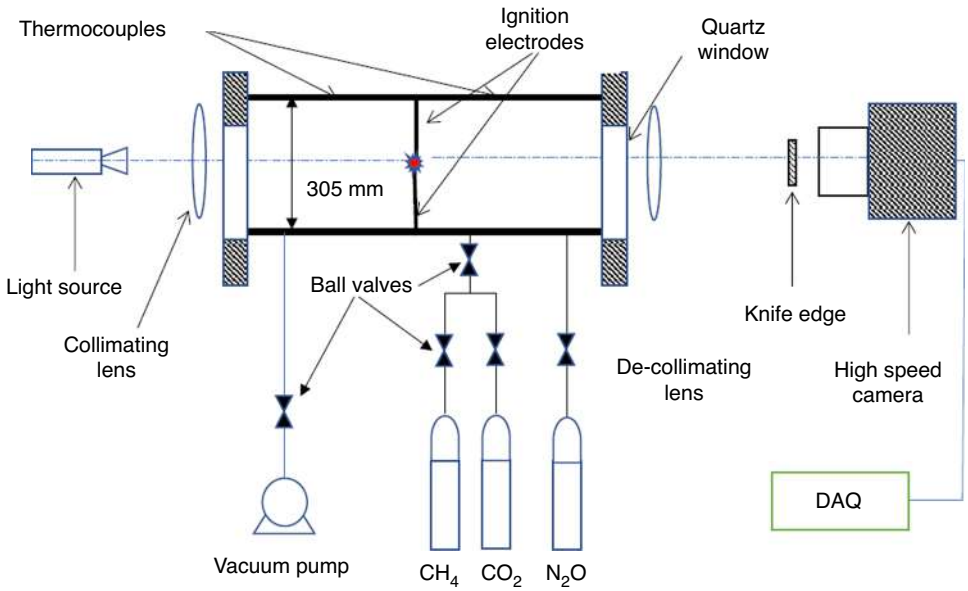

Fig. 1 Experimental setup of constant volume combustion chamber

wall temperature in order to guarantee homogenous combustion temperature. In order to determine the pressure before and after the mixture filling, a digital pressure gauge (Druck DPI 104) is used to adjust the pressure inside the combustion chamber. The total uncertainty of the pressure gauge is 0.01%. Phantom 7.1 is used to take optical recordings of the combustion, the frame rate was set to 5000fps, and the captured images were analyzed using MATLAB software. The partial pressure filling method is utilized to compute the equivalence ratio for each mixture.

Biogas/N_2O mixtures are measured with different CH_4/CO_2 concentrations within various ranges of equivalence ratios. The methane concentration was varied from 75 to 65% while the CO_2 percentages were between the ranges of 25% and 35%. The experiments are conducted at a temperature of 303 K and an atmospheric pressure within an equivalence ratio range of 0.6 to 1.4. The overall uncertainties of the laminar burning velocities are estimated to be around 2.3–6%.

In order to specify the uncertainty in the experiments, bias and accuracy errors were included by conducting five repeated tests for each experiment. Both systematic and random uncertainties were estimated for the experiments. As shown in Table 1, uncertainties are divided into systematic (Si) and random uncertainties (Ri). The calculated standard deviation was then multiplied by the t-distribution for 4 degrees of freedom ($v = n - 1$) and a 95% of confidence interval (CI), before being divided by the square root of n.

The uncertainty in the calculated laminar burning velocity could be described by:

Table 1 List of uncertainties sources

Elemental uncertainty source	Systematic, Si	Random, Ri
Pressure gauge Accuracy Display resolution/bar	± 0.05% F.S	0.0001
Thermocouple K-type Display resolution	1 K	
Camera resolution Finite pixel/cm Spatial/cm	0.057 0.018	
Optical aberration Spatial /cm	0.046	
Calibration Resolution/cm		0.023

$$U_{u_L} = \sqrt{B_{u_L}^2 + \left(\frac{t_{n-1,95}\mathrm{SD}_{u_L}}{\sqrt{n-1}}\right)^2}\,(95\%) \tag{4}$$

where U_{u_L} denotes the uncertainty in the calculated laminar burning velocity at 95% CI, $S_{u_L}^2$ refers to the total bias uncertainty, $B_{u_L}^2$ is the total bias uncertainty, n represents the number of repetitions of the experiment at same condition, while SD_{u_L} denotes the standard deviation, and $t_{n-1,95}$ is the t-distribution value at a 95% CI and $n-1$ degrees of freedom.

Bias uncertainty B_{u_L} on the other hand is determined using the following equation:

$$B_{u_L} = \sqrt{\sum_{i=1}^{N} \left(\frac{\partial u_L^0(x_i)}{\partial x_i} U_i \right)^2} \quad (5)$$

where U_i are the elemental bias uncertainties listed in Table 1; $u_L^0(x_i)$ is a function that expresses the laminar burning velocity as a function of equivalence ratio, initial pressure, initial temperature, optical aberrations, and x_i signifies each elemental error source. Therefore, based on Eq. (5), $u_L^0(x_i)$ should first be determined to solve for the partial derivative $\frac{\partial u_L^0(x_i)}{\partial x_i}$. Sharma et al. [28] proposed a correlation for $u_L^0(x_i)$ which is expressed as:

$$u_L^0 = f(\phi)\left(\frac{T}{303}\right)^{1.68/\sqrt{\phi}} \text{ for } \varphi < 1 \quad (6)$$

and

$$u_L^0 = f(\phi)\left(\frac{T}{303}\right)^{1.68\sqrt{\phi}} \text{ for } \varphi > 1 \quad (7)$$

$$\text{with } f(\phi) = -418 + \frac{1287}{\phi} - \frac{1196}{\phi^2} + \frac{360}{\phi^3} - 15\phi \log_{10} P \quad (8)$$

where T and P are the temperature and pressure, respectively. Ijima and Takeno [29] proposed a much more complex correlation that is given by:

$$u_L^0 = S_{su}\left[1 + \beta \log\left(\frac{P}{P_0}\right)\right]\left(\frac{T}{T_0}\right)^{\alpha} \quad (9)$$

where P_0 and T_0 are the reference temperature with a value of 1 atm and 291 K, respectively. S_{su}, α and β are function of φ with:

$$S_{su} = 36.9 - 210(\phi - 1.12)^2 - 335(\phi - 1.12)^3 \quad (10)$$

$$\alpha = 1.60 - 0.22(\phi - 1) \quad (11)$$

$$\beta = -0.42 - 0.31(\phi - 1) \quad (12)$$

Computational methods

The PREMIX model in CHEMKIN-PRO software is used to predict the laminar burning velocities for the simulated biogas/N_2O mixtures. The unburned conditions were specified according to the initial conditions of the experiments. A multicomponent model is used in order to evaluate the transport properties. The maximum calculation steps were set to be 1000, and the adaptive grid control based on solution gradient was reduced to 0.01.

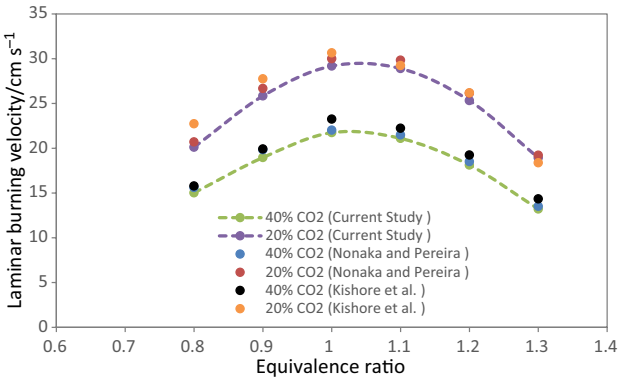

Fig. 2 Comparison between current data and data in literature of the laminar burning velocity of simulated biogas/air mixture of at 1 atm and 298–330 K

Two reaction mechanisms are studied in the present work: GRI-Mech 3.0 and San Diego. The GRI-Mech 3.0 is a mechanism that is extensively used in numerous studies with good results for methane and natural gas studies [9, 10, 30]. San Diego mechanism is designed to focus on high-temperature ignition and detonations studies; the mechanism is adapted to include the nitrogen chemistry in order to calculate the N_2O reactions. The number of reactions in GRI-Mech 3.0 and San Diego mechanisms is 325 and 311, respectively.

Results and discussion

Validation of methodology

In order to validate the reliability of the spherical propagation flame method in a constant volume chamber, the measured LBV was compared with experimental data in the literature [30] and [31]. Due to the lack of studies of biogas/N_2O, the LBVs of simulated biogas/air are illustrated in Fig. 2 over different equivalent ratios at 298 K and 1 atm. The results show a good agreement with literature data; however, the values of LBVs in [31] are slightly higher than the current measurement due to temperature differences (330 K and 1 atm).

Stretch rate and flame speed variation

The unstretched flame speed can be calculated using linear extrapolation of the flame speed and the stretch curve [32]. Flame speed has been investigated by analyzing the images of the spherical flame propagation captured by the high-speed camera (Phantom 7.1) during the combustion by using MATLAB software. Stretch can be calculated by the following equation:

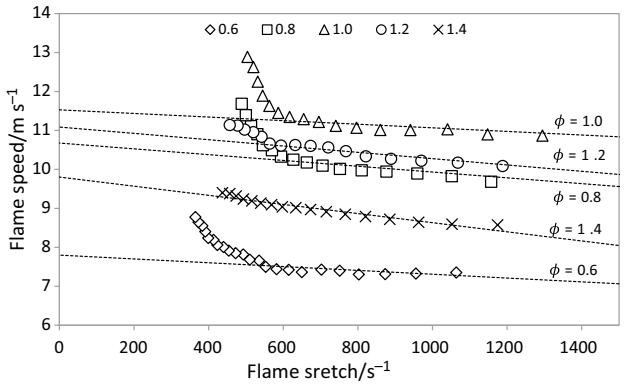

Fig. 3 Flame speed versus flame stretch rate of (75%CH_4/25%CO_2)/N_2O mixture at different equivalence ratios

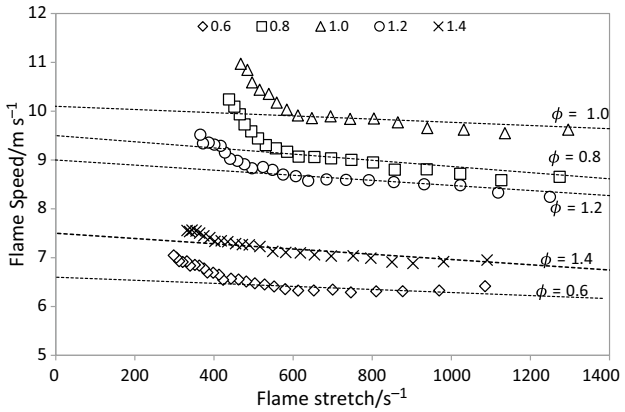

Fig. 4 Flame speed versus flame stretch rate of (65%CH_4/35%CO_2)/N_2O mixture at different equivalence ratios

$$\alpha = \frac{1}{A_f}\frac{dA_f}{dt} = \frac{2}{R_f}\frac{dR_f}{dt} \tag{13}$$

In order to simulate biogas combustion, the flame propagation was studied for different concentrations of (CH_4/CO_2), where the CH_4 percentages in the biogas were set at 65% and 75%, while the percentages of CO_2 were set at 25% and 35%. Experiments were carried out at a temperature of 303 K and atmospheric pressure, with equivalence values ranging from 0.6 to 1.4.

Figures 3 and 4 reveal the correlation between the stretched flame speed and flame stretch rate for two different mixtures of biogas (75%CH_4/25%CO_2)/N_2O and (65%CH_4/35%CO_2)/N_2O at various ranges of equivalence ratios. For all mixtures, the flame propagation speed increased as the stretch rate decreased, which refers to the appositive values of the Markstein length. However, a sudden increase in the flame speed can be observed at lean-to stoichiometric mixtures. The significant acceleration in the flame speed occurs in conjunction with the onset of the cellular instability. Due to the fact that the local stretch rate and the flame area are unknown following the beginning of cellular instability, the LBVs were calculated only within the range of stable flame.

Laminar burning velocity and Markstein length of biogas / N_2O

The experimental results of LBVs of the simulated biogas with nitrous oxide at different concentrations of CH_4/CO_2 are illustrated in Fig. 5 at various ranges of equivalence ratio. The results exhibit a parabolic relation of LBVs versus the equivalence ratio, where the velocities increase from the fuel-lean region until reaching the peak values at the stoichiometric region; then, the values tend to decrease in the fuel-rich region. In general, the values of LBVs tend to decrease with CO_2 increment which acts as a dilutant in biogas; however, the rate of decline is more prominent in the fuel-rich mixture than a fuel-lean mixture that shifting the peak values of LBVs toward leaner mixtures with the increase in CO_2 proportion. These results are thought to be due to the domination of N_2O decomposition reaction in the lean mixture, which produces high energy which leads to increase the burning rate and reduce the dilution effect of CO_2. The summary of the experimental results of LBVs is shown in Table 2.

Figure 6 depicts the spherical flame development of (75% CH_4-25% CO_2)/N_2O, and (65% CH_4-35% CO_2)/N_2O flames which represent the maximum and minimum CO_2 content of the measured flames at the stoichiometric conditions. It is clear that the flame of (75% CH_4-25% CO_2)/N_2O progresses at a higher rate compared to the flames of (65% CH_4-35% CO_2)/N_2O due to the increase in the dilution effect of CO_2. Figure 7 illustrates the development of spherical flame propagation in the mixture of (75% CH_4/25% CO_2)/N_2O over time at various equivalence ratios. The highest rate of flame propagation occurs at the stoichiometric mixture, where the flame is fully formed before reaching the cylinder wall at $t = 5$ ms. The formation of cellularity inside the spherical flame is observed in the lean-to-stoichiometric region, revealing a high impact of the flame instability in this region; however, at $\varphi = 1.4$, the flame propagates smoothly with no cellular formation, indicating less influence of the flame instability in rich mixtures.

The comparison between the experimental results and the prediction results of the LBVs by using GRI 3.0 and San Diego mechanisms is shown in Fig. 8. Compared with the experimental results, both mechanisms showed underestimated values of LBVs, where the experimental data were higher than 10% at stoichiometry compared to GRI 3.0 mechanism and 25% compared to San Diego; however, the GRI 3.0 model provided a better prediction of the LBVs behavior of the experimental results, unlike the

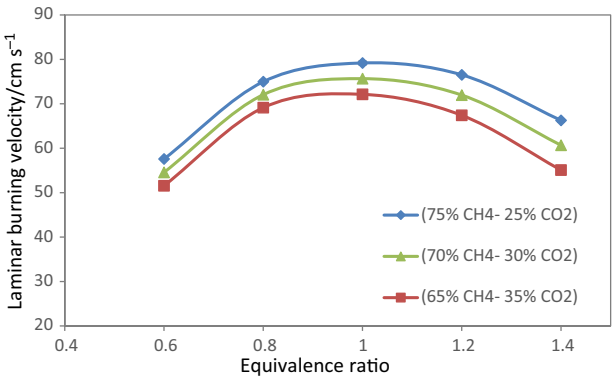

Fig. 5 Laminar burning velocity of simulated biogas/N_2O mixtures

San Diego mechanism that revealed a rich shift of the peak LBV, indicating that the GRI mechanism can be used to examine the influences of N_2O and CO_2 on the combustion of the biogas/N_2O mixture quantitatively. The large divergence between GRI 3.0 and San Diego mechanisms is thought to be due to the limited N_2O reactions of the San Diego mechanism(53 reactions) compared with the GRI3.0 mechanism (106 reactions) [33]. In addition, the divergence in LBV is smaller for rich mixtures and larger for leaner mixtures. Such behavior might be due to the radiation reabsorption influence compelled by the significant portions of N_2 in lean mixtures [34], which is not incorporated in the simulation.

Markstein length is considered as a parameter to evaluate the response of flame to flame stretch rate [35]. Low Markstein length indicates a low influence of flame stretch rate on the burning speed. Figure 9 reveals the behavior of Markstein length over various ranges of equivalent ratios for different compositions of simulated biogas with nitrous oxide. The figure shows that the flame stretch rate for the simulated biogas/N_2O flames near-to-stoichiometric ratio has little effect on the stretched flame speed, whereas it has a larger effect on the flame speed for fuel-lean and fuel-rich mixtures. The Markstein length is also used to estimate the mixture sensitivity to flame instability. The lower Markstein length means the earlier onset of flame instability. It is found that the increase in CO_2 percentage leads to an increase in Markstein length. Thus, the instability of flames begins earlier for (75% CH_4, 25% CO_2)/N_2O mixture than that of (65% CH_4, 35% CO_2)/N_2O.

Figure 10 compares the behavior of the experimental laminar burning velocities of biogas/N_2O and biogas/air at a temperature of 303 K and atmospheric pressure at various equivalence ratios with an identical composition of biogas (65%CH_4/35%CO_2). Figure 10 shows a significant increase in LBV values for biogas/N_2O mixture compared to biogas/air mixture, where the values of LBVs increased by about 335% at $\varphi = 0.8$ and by about 211% at $\varphi = 1.0$, indicating a significant influence of N_2O chemical reactions in improving the laminar burning velocity values. With such a significant increase in LBV values, biogas/N_2O may be considered as an interesting mixture to be used in the propulsion applications that requires high burning combustion.

Table 2 Summary of LBVs experimental results at 303 K and atmospheric pressure

	Eq. Ratio	S_L/cm s^{-1} 75%CH_4-25%CO_2	S_L, Av/cm s^{-1} 75%CH_4-25%CO_2	S_L/cm s^{-1} 65%CH_4-35%CO_2	S_L, Av/cm s^{-1} 65%CH_4-35%CO_2
Test 1	0.6	57.87	57.57	51.54	51.54
Test2	0.6	57.51		51.49	
Test3	0.6	57.33		51.60	
Test 1	0.8	74.64	74.97	69.19	69.13
Test2	0.8	75.00		68.94	
Test3	0.8	75.28		69.26	
Test 1	1.0	78.76	79.19	71.79	72.12
Test2	1.0	79.67		72.08	
Test3	1.0	79.14		72.51	
Test 1	1.2	76.63	76.52	67.15	67.40
Test2	1.2	76.32		67.87	
Test 3	1.2	76.61		67.19	
Test 1	1.4	66.22	66.27	55.13	55.07
Test2	1.4	66.68		55.28	
Test3	1.4	65.92		54.81	

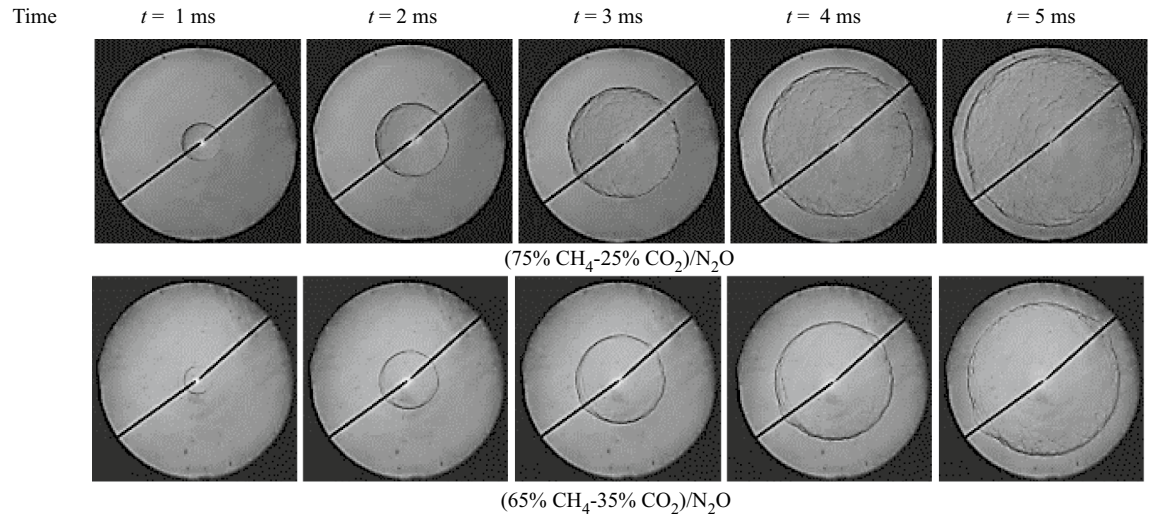

Fig. 6 Development of spherical flame for different concentrations of biogas/N_2O mixtures at the stoichiometric condition

Hydrodynamic instability

Hydrodynamic instability is heavily influenced by the thermal expansion [36], which can be identified by the thermal expansion ratio (σ) and flame thickness (δ_T). The thermal expansion ratio (σ) is defined as the ratio of unburned gas density to that of burned gas (ρu/ρb); the higher the density jump is, the higher the flame instability [35]. Flame thickness (δ_T) can be determined by the temperature profile of the flame structure and can be calculated by the following equation:

$$\delta_T = \frac{\lambda}{c_p \rho_u u_l} \tag{14}$$

where λ and c_p are the thermal conductivity and specific heat at constant pressure of biogas unburned mixture.

The flame thickness has a strong influence on hydrodynamic instability. The strong stretch effect on the flame-front has an inhibition effect on the development of cellular for the spherical flame propagation which has positive curvature, and therefore, a reduction in flame thickness will weaken the influence of curvature and the instability tendency becomes stronger.

Figure 11 illustrates the behavior of the flame thickness of the biogas/N_2O mixtures at a different range of equivalence ratios using Gaseq chemical equilibrium software. The figure shows a parabolic behavior in the value of flame thickness with the equivalence ratio. For all mixtures, the values of flame thickness are decreasing gradually with increasing the equivalence ratio at the lean-to-stoichiometric region, whereas it shows an apparent increase at the stoichiometric-to-rich region, which indicates that the influence of curvature on the flame front is weakened at the lean-to-stoichiometric region; thus, the instability propensity of the flame is increased, while the influence of curvature on the flame front is enhanced at the fuel-rich region. It was also found that the higher the percentage of CO_2 concentration in biogas/N_2O increased the flame thickness. The flame thickness trend reveals an inverse relation with the experimental results of laminar burning velocity, suggesting that the decrease in flame thickness increases the laminar burning velocity. The flame instability increases from lean-to-stoichiometric mixtures, while the flame tends to be more stable at rich mixtures. Such behavior is noticed in Fig. 7 where the formation of the cellularity is diminished at rich mixtures.

The adiabatic flame temperatures of different biogas/N_2O mixtures have been calculated numerically for various ranges of equivalence ratios at an initial temperature of 303 K and atmospheric pressure. Figure 12 depicts that the behavior of the flame temperature is consistent with that of the laminar burning velocities, where the peak temperature value is at the stoichiometric region. The higher CO_2 content in biogas decreases the adiabatic flame temperatures values due to the increase in the dilution effect.

Figure 13 shows the effect of equivalence ratio variation with the density ratio of unburned gas density to that of burned gas for different mixtures of simulated biogas/N_2O ratios using Gaseq chemical equilibrium software. The values of the density ratio show a considerable increase at lean-to-stoichiometric region causes a significant variation in the flame front's thermal expansion effect, which increases the hydrodynamic instability at this region, while the variation in the density ratio is minimal at the stoichiometric-to-rich region, which indicates a little effect of the flame front's thermal expansion.

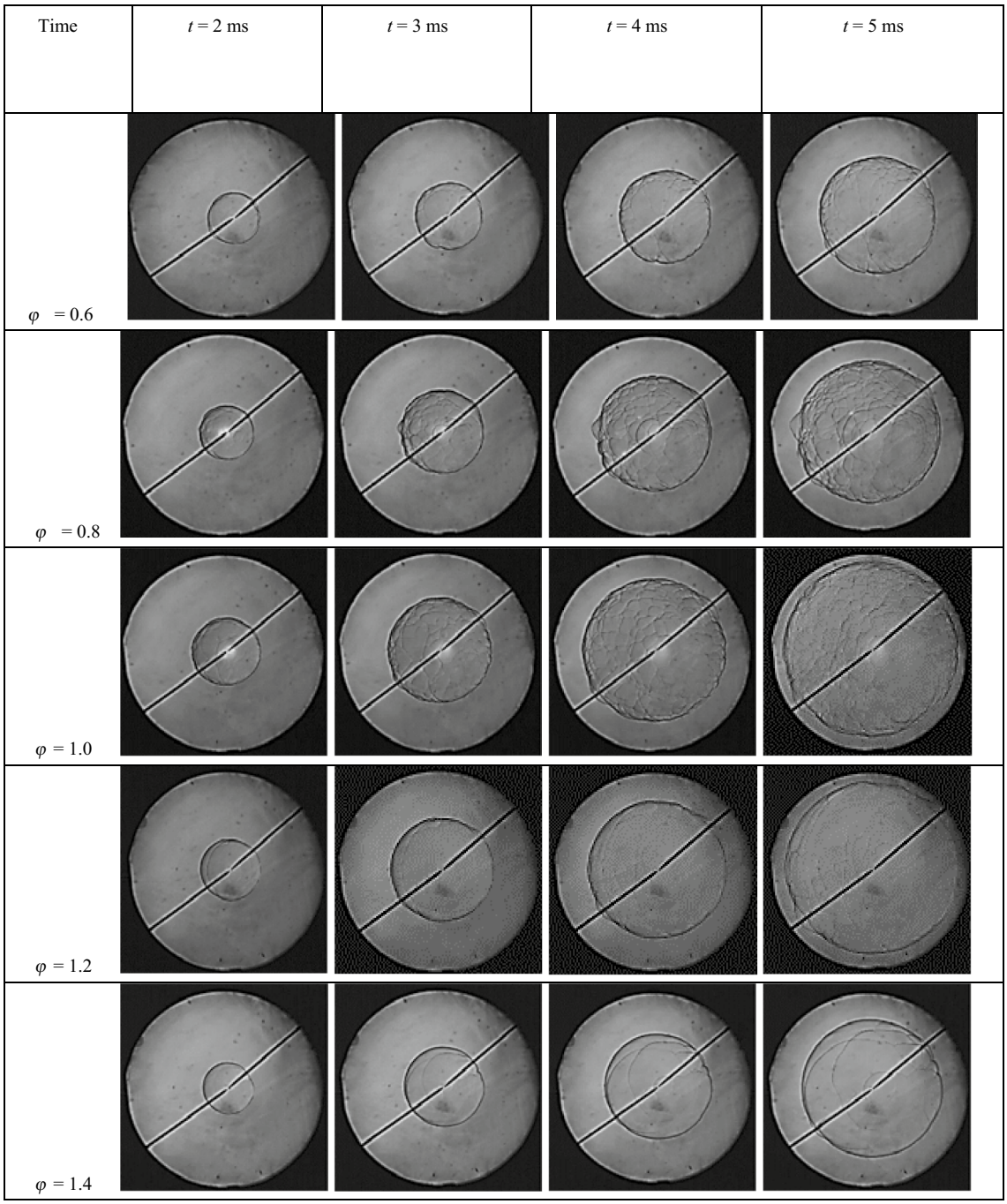

Fig. 7 Development of spherical flame of $(75\%CH_4/25\%CO_2)/N_2O$ mixture at different equivalence ratios

Diffusive–thermal instabilities

Cellular instability in premixed flames can be generated by hydrodynamic and/or diffusive–thermal instabilities, which lead to local flame acceleration [14].

Thermal diffusivity (α_T) is defined in heat transfer analysis as the ratio between thermal conductivity (λ) divided by the density and specific heat at constant pressure. Thermal diffusivity (α_T) can be calculated by the following equation:

$$\alpha_T = \frac{\lambda}{c_p \rho_u} \tag{15}$$

Figure 14 depicts the correlation between the thermal diffusivity values with a wide range of equivalence ratios

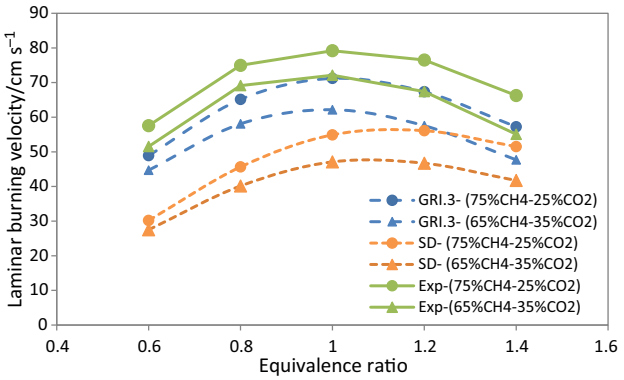

Fig. 8 Comparison between the experimental results and predicted results of LBVs of simulated biogas/N_2O

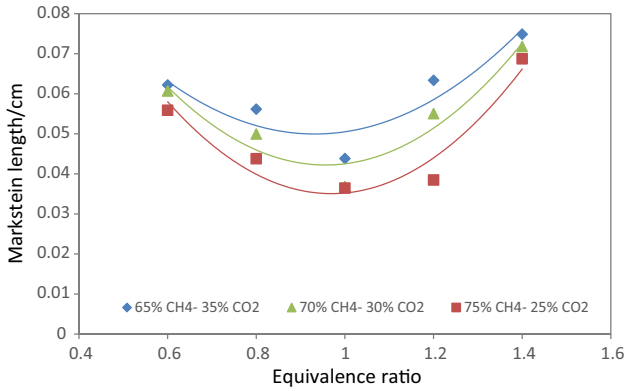

Fig. 9 Markstein length of different concentrations of biogas/N_2O mixtures

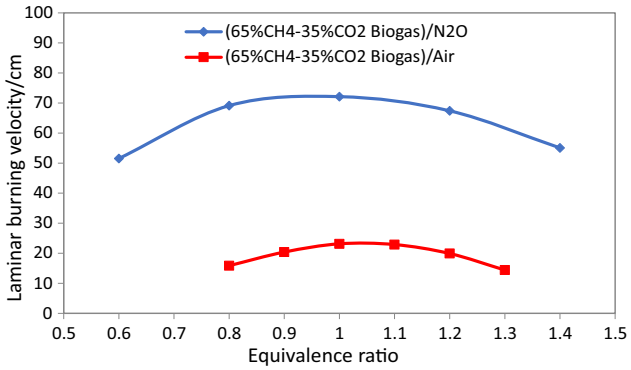

Fig. 10 Comparison of laminar burning velocities of biogas/N_2O and biogas/air at different equivalence ratios

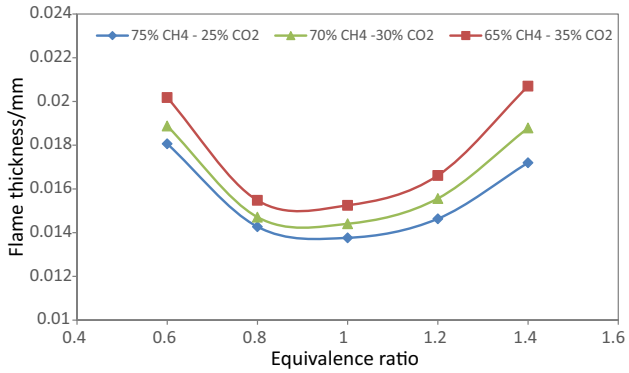

Fig. 11 Flame thickness of different concentrations of biogas/N_2O mixtures

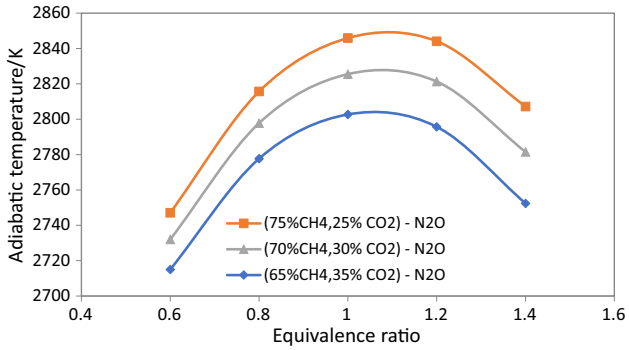

Fig. 12 Adiabatic flame temperature of different concentrations of biogas/N_2O mixtures

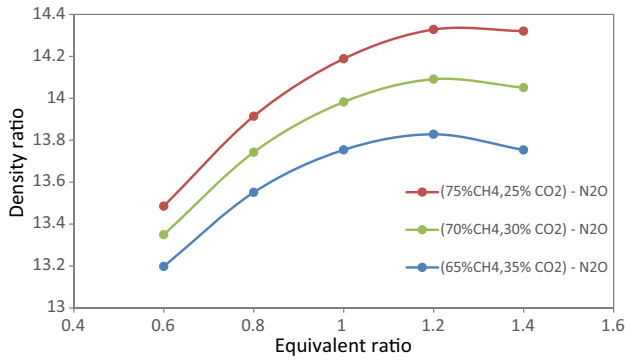

Fig. 13 Density ratio of different concentrations of biogas/N_2O mixtures

using Gaseq chemical equilibrium software. A direct proportional relation of the thermal diffusivity values versus the equivalence ratios is observed, indicating that thermal diffusivity is significantly affected by fuel proportion, i.e., biogas. In addition, the thermal diffusivity values decrease with the increase in the carbon dioxide content in biogas due to the dilution effect of CO_2; however, CO_2 increment showed no effect on the thermal diffusivity values at the stoichiometric ratio and the rich mixture of $\varphi = 1.4$. With regard to comparing the behavior of thermal diffusivity with the experimental results of laminar burning velocity, the effect

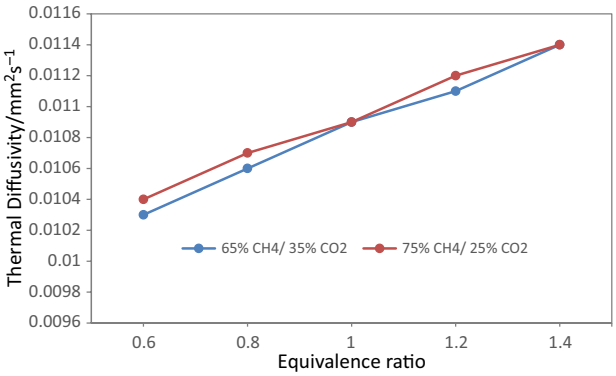

Fig. 14 Thermal diffusivity of different concentrations of biogas/N_2O mixtures

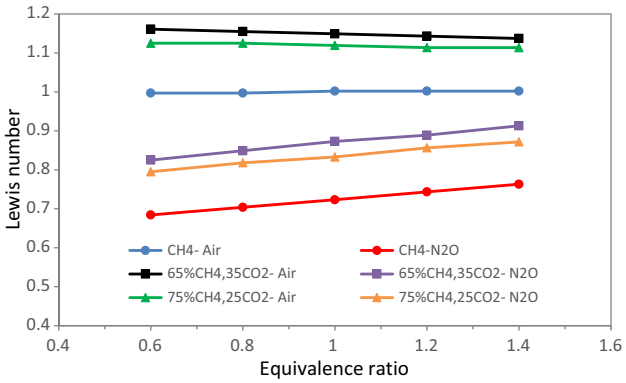

Fig. 15 Comparison of Lewis number for pure methane and different concentrations of biogas with N_2O and air

of thermal diffusivity is directly proportional to the laminar burning velocity at the lean-to-stoichiometric ratios, where the velocity increases with the increase in thermal diffusivity. In contrast, the velocity decreases with the increase in thermal diffusivity at rich mixtures.

Lewis number (L_e) is a dimensionless number which is defined as the ratio of thermal diffusivity to mass diffusivity. Lewis number can be roughly evaluating the diffusive–thermal instability. When $L_e < 1$, the flame instability increases; while $L_e > 1$, the flame instability decreases.

Lewis number can be estimated by the following equation:

$$L_e = \frac{D_T}{D_m} = \frac{\lambda}{C_p \rho_u D_m} \tag{16}$$

where D_T is the thermal diffusivity, D_m is the mass diffusivity, λ is the heat conductivity, and ρ_u is the density of unburned reactant and C_p is the specific heat at constant pressure.

Lewis number characterizing mixtures with a single fuel that contains a dilute such as CO_2 in biogas was expressed as:

$$L_e = \frac{D_T}{\boldsymbol{D}i,\ \text{mix}} \tag{17}$$

where $\boldsymbol{D}i$, mix denotes the mass diffusivity as the fuel–oxidizer mixture only consisted of fuel i and oxidizer (and any diluents) [37, 38].

The addition of inert species such as CO_2 in biogas promotes flame extinction; however, it may also alter the diffusive–thermal properties of fuel and oxidizer flows, which have a strong influence on the temperature and extinction of the flames [39].

Figure 15 illustrates the value of Lewis number for pure methane and different compositions of biogas with nitrous oxide and air as oxidizers at different equivalence ratios. For fuel/N_2O mixtures, it is found that the relation of the Lewis number versus equivalence ratio is directly proportional where Lewis's number increases with the increase in the equivalent ratio; however, the figure shows that Le < 1 throughout all equivalence ratios range, which indicates that the diffusive–thermal instability is dominant for all N_2O mixtures. For CH_4/air mixture, the Lewis number value is almost constant where the values of Le ≈1 at the calculated range of equivalence ratios, indicating a minor effect of the thermo-diffusive instability on the flame. For the biogas/air mixtures, the value of the Lewis number is higher than unity, with a slight decrease in Lewis number with the increase in equivalence ratio, indicating that the diffusive thermal instability stabilizes the flame. The CO_2 increment increases the Lewis number values for all mixtures, which means that the increase in the percentage of CO_2 in biogas diminishes the influence of the diffusive–thermal instabilities.

From the investigation of the hydrodynamic and diffusive–thermal instabilities, it can be noticed that the flame instability for biogas/N_2O mixtures is caused by the combined influences of hydrodynamic and diffusive–thermal instabilities, particularly in lean-to-stoichiometric mixtures, where the flame thickness decreases and Le < 1with a minor influence of thermal diffusivity, while in rich mixtures, the effect of flame instability decreases due to the increase in flame thickness and Lewis number with the increase in equivalence ratio.

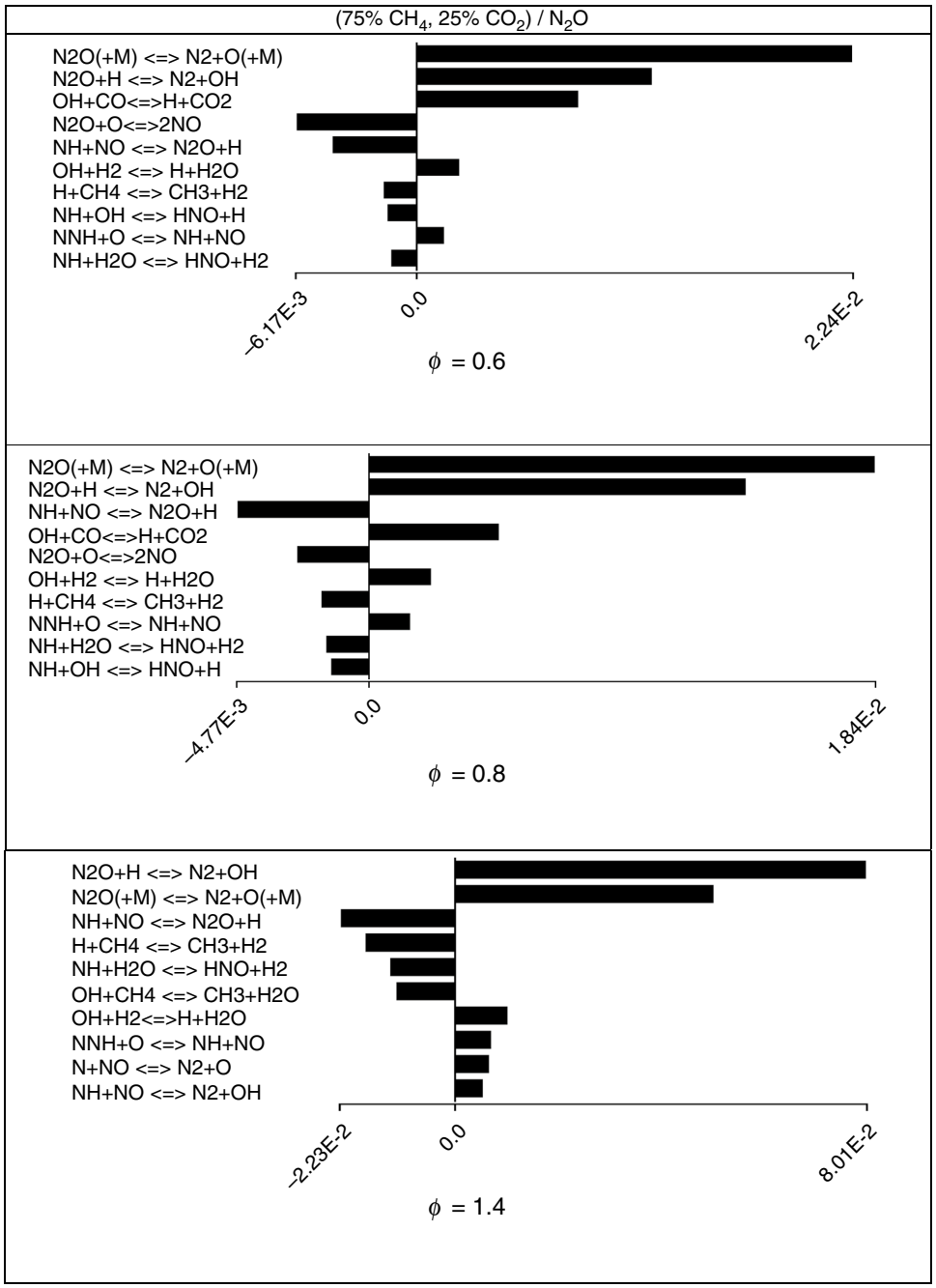

Fig. 16 Normalized sensitivity analyses of (75% CH_4, 25% CO_2)/N_2O for different equivalence ratios at 303 K

Sensitivity analysis

In order to comprehend the influence of chemical reactions on the LBVs of biogas/N_2O, the detailed chemical kinetics mechanism for (75% CH_4, 25% CO_2)/N_2O and (65% CH_4, 35% CO_2)/N_2O reactions has been established at various equivalence ratios $\varphi = (0.6–1.4)$ using CHEMKIN-PRO at a temperature of 303 K and an atmospheric pressure.

Normalized sensitivity coefficients of the top 10 elementary reactions for (75% CH_4, 25% CO_2)/N_2O and (65% CH_4, 35% CO_2) / N_2O are shown in Figs. 16 and 17, respectively. It is clear that the most important reactions vary with the equivalence ratios. As shown in both figures,

Fig. 16 (continued)

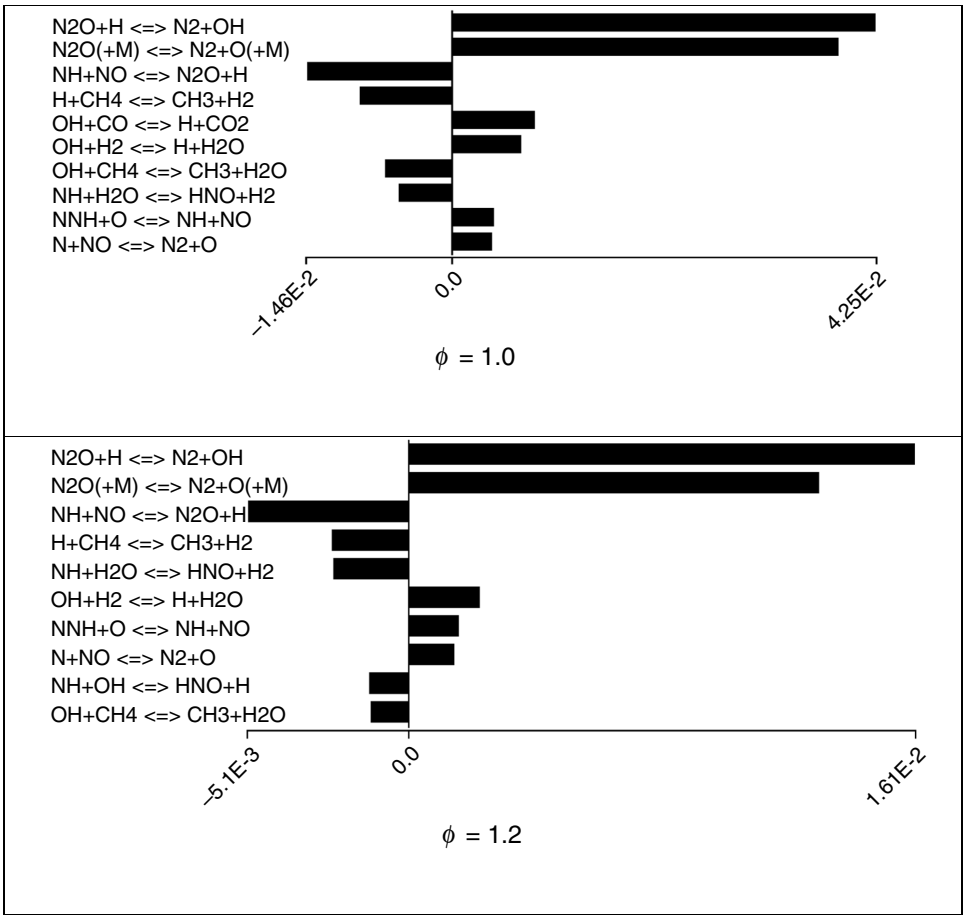

the most important promoting reaction is $N_2O(+M) \Leftrightarrow N_2 + O(+M)$ (R1) for case $\varphi = 0.6$ and 0.8, which is an endothermic reaction. The reaction of biogas/N_2O is therefore dominated by such an endothermic reaction of N_2O decomposition. Nevertheless, the most important reaction is $N_2O + H \Leftrightarrow N_2 + OH$ (R2) for case $\varphi = 1.0$, 1.2, and 1.4, and the reaction (R1) locates at the second significant position. Therefore, the influence of thermal decomposition reaction (R1) on LBV is restrained correspondingly. On the other hand, the reaction $N_2O + O \Leftrightarrow 2NO$ (R4) due to sufficient oxidizer at fuel-lean mixtures is competing to some extent with the endothermic reactions (R1) and (R2) for the consumption of N_2O, particularly at lean mixtures. It can be seen that the N_2O decomposition reaction $N_2O(+M) \Leftrightarrow N_2 + O(+M)$ (R1) always exists in the biogas/N_2O mixtures and it is a dominant reaction in lean mixtures. This analysis reveals the influence of N_2O consumption reactions on the significant increase rate of LBVs at lean mixtures.

However, for all investigated biogas/N_2O mixtures, the laminar burning velocity is highly influenced by the rate of H attack on N_2O (R2), producing N2 and OH, where the sensitivity of (R2) increases from the fuel-lean region until reaching the peak values at the stoichiometric region, followed by a gradual decrease at the fuel-rich region, similar to LBV behavior. The significant effect of the $N_2O + H \Leftrightarrow N_2 + OH$ reaction on LBV was also indicated in other CH_4/N_2O investigations [40].

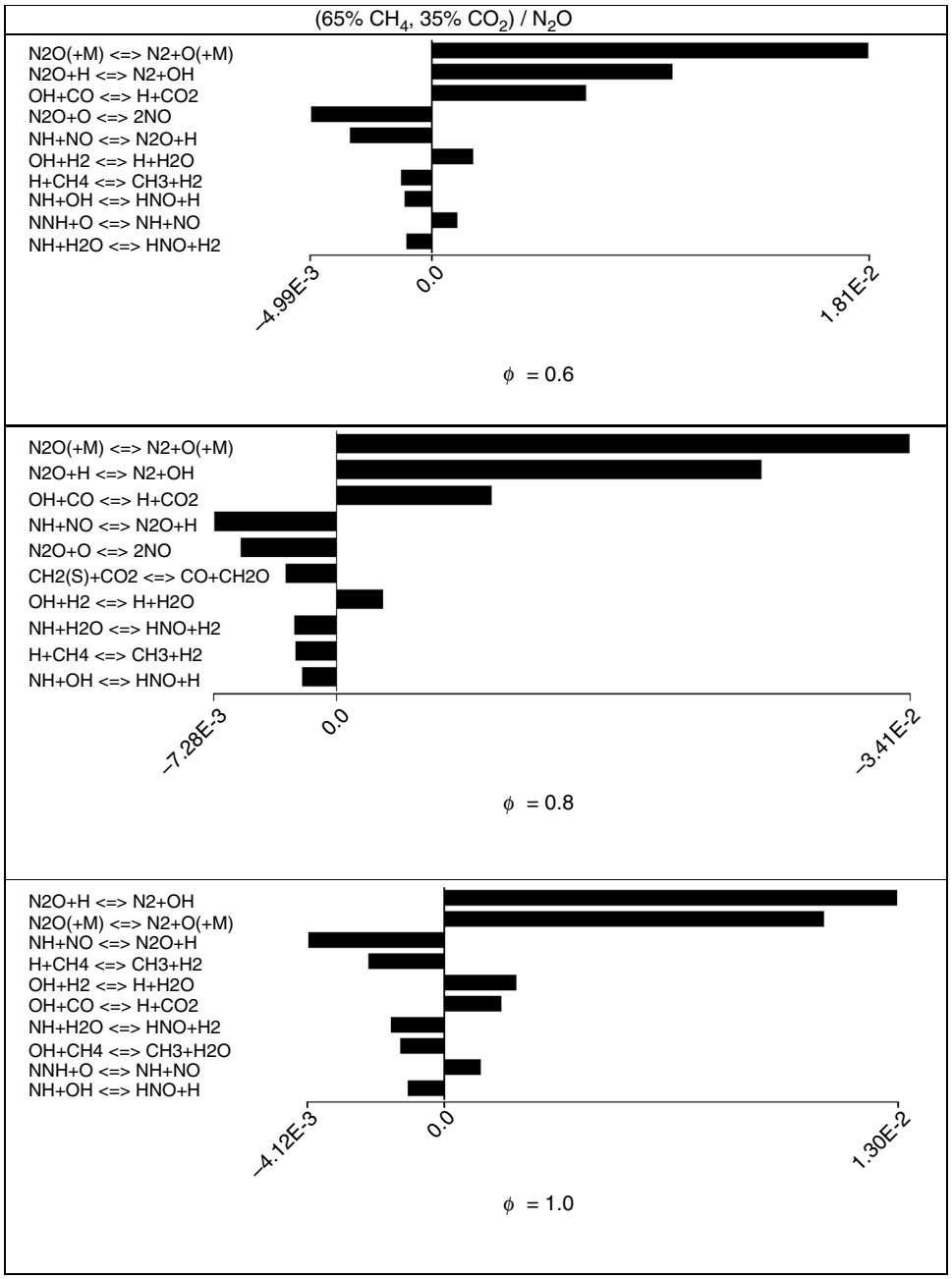

Fig. 17 Normalized sensitivity analyses of (65% CH_4, 35% CO_2)/N_2O for different equivalence ratios at 303 K

Fig. 17 (continued)

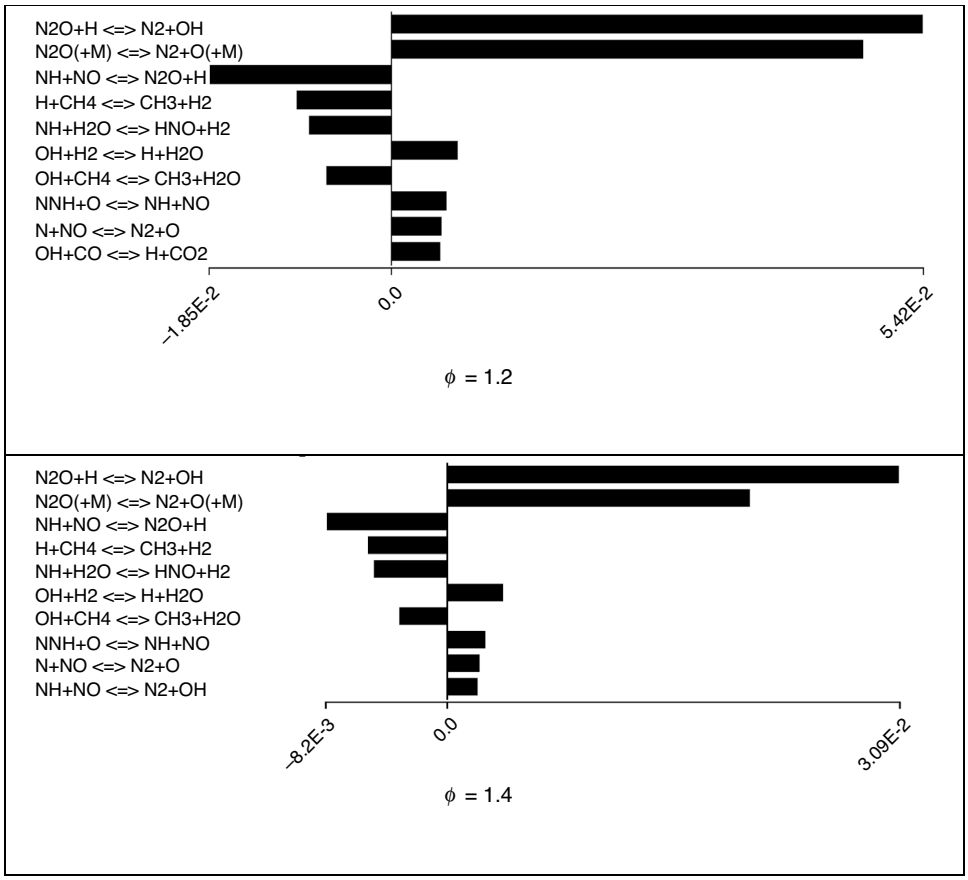

Conclusions

In the present study, the laminar burning velocities and flame stability for different concentrations of biogas/N_2O flames were measured experimentally and numerically over a wide range of equivalence ratios at a temperature of 303 K and atmospheric pressure. In light of the present study, the following conclusions may be drawn:

(1) The methodology validation for the current study is carried out using biogas/air against other literature data and the experimental results showed a good agreement with other experimental data available in the literature.
(2) The experimental data of LBVs showed a parabolic relation versus the equivalence ratio, where the peak values of LBVs are located at the stoichiometric region. The LBVs decrease as the CO_2 proportion in biogas/N_2O increases; however, the decline rate is prominent in the fuel-rich region than in the fuel-lean region.
(3) At the same conditions, the experimental results of LBVs were compared to the LBVs prediction data of GRI 3.0 and San Diego mechanisms. Both mechanisms provided lower LBVs prediction values, however, the GRI 3.0 model showed the nearest LBVs prediction to the experimental results.
(4) It is found that lower Markstein length values are located near to the stoichiometric ratio, thus, the flame stretch rate has little effect on the stretched flame speed at the stoichiometric region. The higher CO_2 percentage in the biogas/N_2O mixture increases the Markstein length. Therefore, the occurrence of flame instability begins earlier with CO_2 reduction in biogas/N_2O mixture.
(5) Due to the decrease in flame thickness, the influence of curvature on the flame front is weakened at the fuel lean-to-stoichiometric region; therefore, the flame instability tends to increase in this region, while the flame instability tends to decrease in the stoichiometric-to-rich region. It is found that CO_2 increment in biogas/N_2O mixture increases the flame thickness.
(6) The thermal diffusivity is significantly influenced by the fuel proportion in biogas/N_2O mixtures. The thermal diffusivity values decline with increasing the CO_2% in biogas due to its dilution effect. However, CO_2 increment revealed no impact on the thermal diffusivity values at $\varphi = 1.0$ and $\varphi = 1.4$.
(7) Lewis number values for CH_4/N_2O and biogas/N_2O mixtures were below the unity throughout the range of the estimated equivalences ratios, which implies that the diffusive–thermal instability is dominant for

all N_2O mixtures. The CO_2 dilution in the biogas/N_2O increases the values of Lewis number, which indicates a reduction in the diffusive–thermal instabilities with CO_2 increment. It is found that the higher the equivalence ratio increases the Lewis number in a direct proportional relation.

(8) The nitrous oxide decomposition reaction $N_2O(+M) \Leftrightarrow N_2 + O(+M)$ is the most powerful reaction in biogas/N_2O combustion at the fuel-lean region, while the influence of N_2O decomposition is weakened at the stoichiometric-to-rich region; consequently, there is the shifting of the values of LBVs toward leaner mixtures with CO_2 increment.

Acknowledgements The authors would like to thank Universiti Teknologi Malaysia and Ministry of Higher Education Malaysia for supporting this research activity under the Research Grant Scheme No. Q.J130000.3551.07G58 and Q.J130000.3551.07G14.

References

1. Pizzuti L, Martins CA, Lacava PT. Laminar burning velocity and flammability limits in biogas: a literature review. Renew Sustain Energy Rev. 2016;62:856–65.
2. Elhawary S, Saat A, Wahid MA, Ghazali AD. Experimental study of using biogas in Pulse Detonation Engine with hydrogen enrichment. Int J Hydrogen Energy. 2020;45(30):15414–24.
3. Xin Z, Jian X, Shizhuo Z, Xiaosen H, Jianhua L. The experimental study on cyclic variation in a spark ignited engine fueled with biogas and hydrogen blends. Int J Hydrogen Energy. 2013;38(25):11164–8.
4. Park C, Park S, Lee Y, Kim C, Lee S, Moriyoshi Y. Performance and emission characteristics of a SI engine fueled by low calorific biogas blended with hydrogen. Int J Hydrogen Energy Pergamon. 2011;36:10080–8.
5. Todt D, Dörsch P. Mechanism leading to N2O production in wastewater treating biofilm systems. Rev Environ Sci Biotechnol. 2016;15(3):355–78.
6. Bock E, Wagner M. The prokaryotes. Springer; 2006. p. 457–95.
7. Konnov AA, Mohammad A, Kishore VR, Il KN, Prathap C, Kumar S. A comprehensive review of measurements and data analysis of laminar burning velocities for various fuel+air mixtures. Prog Energy Combust Sci. 2018;68:197–267.
8. Gibbs GJ, Calcote HF, Calcote HF. Effect of molecular structure on burning velocity. J Chem Eng Data. 1959;4:226–37.
9. Hermanns RTE, Konnov AA, Bastiaans RJM, de Goey LPH, Lucka K, Köhne H. Effects of temperature and composition on the laminar burning velocity of CH4 + H2 + O2 + N2 flames. Fuel. 2010;89:114–21.
10. Goswami M, Derks SCR, Coumans K, Slikker WJ, de Andrade Oliveira MH, Bastiaans RJM, et al. The effect of elevated pressures on the laminar burning velocity of methane+air mixtures. Combust Flame. 2013;160:1627–35.
11. Wei Z, Zhen H, Fu J, Leung C, Cheung C, Huang Z. Experimental and numerical study on the laminar burning velocity of hydrogen enriched biogas mixture. Int J Hydrogen Energy. 2019;44:22240–9.
12. Weilong W, Huiqiang Z. Laminar burning velocities of C2H4/N2O flames: experimental study and its chemical kinetics mechanism. Combust Flame. 2019;202:362–75.
13. Askari O, Elia M, Ferrari M, Metghalchi H. Cell formation effects on the burning speeds and flame front area of synthetic gas at high pressures and temperatures. Appl Energy. 2017;189:568–77.
14. Kim HJ, Van K, Lee DK, Yoo CS, Park J, Chung SH. Laminar flame speed, Markstein length, and cellular instability for spherically propagating methane/ethylene–air premixed flames. Combust Flame. 2020;214:464–74.
15. Powell OA, Papas P, Dreyer C. Laminar burning velocities for hydrogen-, methane-, acetylene-, and propane-nitrous oxide flames. Combust Sci Technol. 2009;181:917–36.
16. Jayachandran J, Lefebvre A, Zhao R, Halter F, Varea E, Renou B, et al. A study of propagation of spherically expanding and counterflow laminar flames using direct measurements and numerical simulations. Proc Combust Inst. 2015;35:695–702.
17. Vanderhoff JA, Beyer RA, Kotlar AJ. Laser raman spectroscopy of flames; temperature and concentrations in CH 4/N20 flames us army armament research and development command ballistic research laboratory aberdeen proving ground, Maryland. 1982
18. Habeebullah MB, Alasfour FN, Branch MC. Structure and kinetics of CH4/N2O flames. Symp Combust. 1991;23:371–8.
19. Zabarnick S. Laser-induced fluorescence diagnostics and chemical kinetic modeling of a CH4/NO2/O2 flame at 55 torr. Combust Flame. 1991;85:27–50.
20. Vandooren J, Branch MC, Van Tiggelen PJ. Comparisons of the structure of stoichiometric CH4N2OAr and CH4O2Ar flames by molecular beam sampling and mass spectrometric analysis. Combust Flame. 1992;90:247–58.
21. Powell OA, Papas P, Dreyer CB. Hydrogen- and C1–c3 hydrocarbon-nitrous oxide kinetics in freely propagating and burner-stabilized flames, shock tubes, and flow reactors. Combust Sci Technol. 2010;182:252–83.
22. Pfahl UJ, Ross MC, Shepherd JE, Pasamehmetoglu KO, Unal C. Flammability limits, ignition energy, and flame speeds in H2-CH4-NH3- N2O-O2-N2 mixtures. Combust Flame. 2000;123:140–58.
23. Shebeko AY, Shebeko YN, Zuban' AV, Navtsenya VY, Azatyan VV. Influence on fluorocarbons flammability limits in the mixtures of H 2–N2O and CH4-N2O. Russ J Phys Chem B. 2014;8:65–70.
24. Newman-Lehman T, Grana R, Seshadri K, Williams F. The structure and extinction of nonpremixed methane/nitrous oxide and ethane/nitrous oxide flames. Proc Combust Inst. 2013;34:2147–53.
25. Razus D, Mitu M, Giurcan V, Movileanu C, Oancea D. Methane-unconventional oxidant flames. Laminar burning velocities of nitrogen-diluted methane–N2O mixtures. Process Saf Environ Prot Inst Chem Eng. 2018;114:240–50.
26. Goga G, Chauhan BS, Mahla SK, Dhir A, Cho HM. Effect of varying biogas mass flow rate on performance and emission characteristics of a diesel engine fuelled with blends of n-butanol and diesel. J Therm Anal Calorim. 2020;140:2817–30.
27. Lin Z, Sun D, Dang Y, Holmes DE. Significant enhancement of nitrous oxide energy yields from wastewater achieved by bioaugmentation with a recombinant strain of Pseudomonas aeruginosa. Sci Rep Nature. 2018;8:1–9.
28. Sharma SP, Agrawal DD, Gupta CP. The pressure and temperature dependence of burning velocity in a spherical combustion bomb. Symp Combust. 1981;18:493–501.
29. Iijima T, Takeno T. Effects of temperature and pressure on burning velocity. Combust Flame. 1986;65:35–43.
30. Nonaka HOB, Pereira FM. Experimental and numerical study of CO2 content effects on the laminar burning velocity of biogas. Fuel. 2016;182:382–90.
31. Ratna Kishore V, Duhan N, Ravi MR, Ray A. Measurement of adiabatic burning velocity in natural gas-like mixtures. Exp Therm Fluid Sci. 2008;33:10–6.

32. Gillespie L, Lawes M, Sheppard CGW, Woolley R. Aspects of Laminar and Turbulent Burning Velocity Relevant to SI Engines. SAE Tech Pap SAE International; 2000.
33. Weilong W, Huiqiang Z. Laminar burning velocities of C2H4/N2O flames: Experimental study and its chemical kinetics mechanism. Combust Flame. 2019;202:362–75.
34. Ju Y, Masuya G, Ronney PD. Effects of radiative emission and absorption on the propagation and extinction of premixed gas flames. Symp Combust. 1998;27:2619–26.
35. Li H, Li G, Sun Z, Yu Y, Zhai Y, Zhou Z. Experimental investigation on laminar burning velocities and flame intrinsic instabilities of lean and stoichiometric H2/CO/air mixtures at reduced, normal and elevated pressures. Fuel. 2014;135:279–91.
36. Kwon S, Tseng LK, Faeth GM. Laminar burning velocities and transition to unstable flames in H2/O2/N2 and C3H8/O2/N2 mixtures. Combust Flame. 1992;90:230–46.
37. Lapalme D, Lemaire R, Seers P. Assessment of the method for calculating the Lewis number of H2/CO/CH4 mixtures and comparison with experimental results. Int J Hydrogen Energy. 2017;42:8314–28.
38. Bouvet N, Halter F, Chauveau C, Yoon Y. On the effective Lewis number formulations for lean hydrogen/hydrocarbon/ air mixtures. Int J Hydrogen Energy Pergamon. 2013;38:5949–60.
39. Chen RH, Chaos M, Kothawala A. Lewis number effects in laminar diffusion flames near and away from extinction. Proc Combust Inst. 2007;31:1231–7.
40. Razus D, Mitu M, Giurcan V, Movileanu C, Oancea D. Methane-unconventional oxidant flames. Laminar burning velocities of nitrogen-diluted methane–N2O mixtures. Process Saf Environ Prot. 2018;114:240–50.